

Introduction

Accurate diagnosis of cancer (and other diseases) is hampered by the inability to extract target cells from human biopsy samples. Cancer cells often make up a small fraction of the total number of cells in a biopsy samples. The result is that downstream molecular analyses are confounded by DNA from non-cancer cells, leading to an inability to diagnose (insufficient sample) or worse, misdiagnoses. Expression Microdissection (xMD) is the second generation technology for the problem. Therefore, our goal is to state and simulate the physics behind the process of xMD, shown in Figure 1, so that it can be understood and quantified [1, 2]. We state a thermal model to simulate transient temperature distribution in the xMD media during laser irradiation.

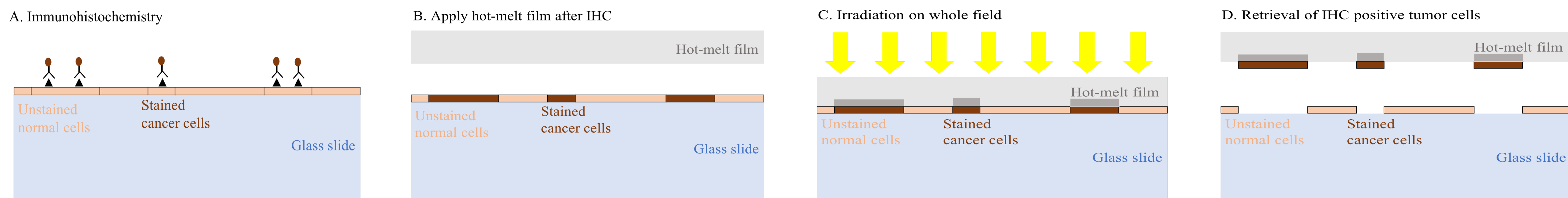


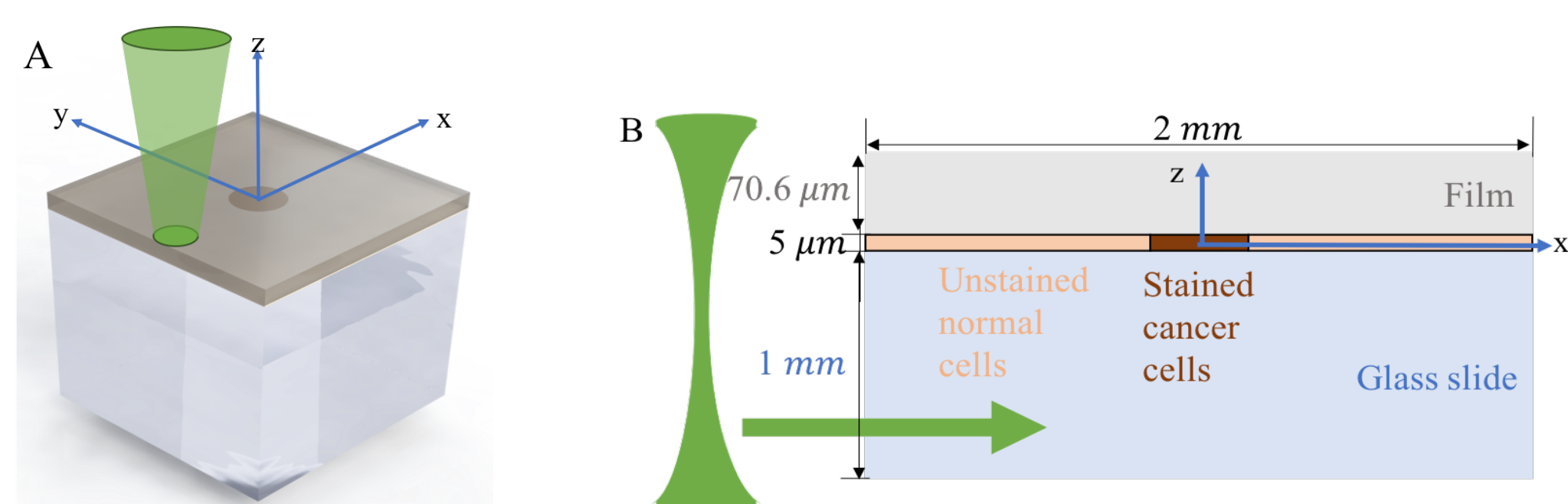
Figure 1 Stepwise schematic of Expression Microdissection developed and patented at NIH [1, 3]

Mathematical Model

The transient temperature distribution in the film, tissue, and glass, during laser irradiation can be estimated by solving a heat transfer equation with a moving heat source due to the scanning laser

$$\rho C \frac{\partial T}{\partial t} = \nabla \cdot (k_c \nabla T) + \frac{2\mu_a P}{\pi r_0^2} \exp\left(-2 \frac{(x - x_f)^2 + y^2}{r_0^2}\right) \exp(-\mu_a z) \quad (1)$$

where $T = T(x, y, z, t)$, ρ is density, C is specific heat, k_c is thermal conductivity, μ_a is absorption coefficient, r_0 is the radius of collimated laser spot, P is the laser power, x_f is the position of the laser spot moving along the x-axis. The **boundary conditions** include i) the symmetry plane at the xz plane; ii) constant room temperature at the bottom of the glass slide and the boundary planes perpendicular to the y-axis; and iii) free air convection at the rest of the boundaries. The **assumptions** used are A) absorption of backscattered light is negligible because both the tissue and film are very thin and have strong forward scattering; B) optical and thermal properties are thermally stable during the process; C) radiation emission from the sample is neglected; and D) there is good thermal contact between the film and the tissue section. COMSOL Multiphysics 5.3 was employed for the solution of the equation (1).



C	ρ (Kg/m ³)	C (J/Kg·K)	K_c (W/m·K)	μ_a (1/mm)
Film	950	3140	0.335	0.24
Tissue	980	3780	0.485	0.07
Stained tissue	980	3780	0.485	28
Glass slide	2230	837	1.088	0

Figure 2A) Schematic of the media scanned by a collimated continuous-wave laser. 2B) Configuration of the media. 2C) Physical properties used for simulation[4, 5, 6, 7, 8].

Results

The simulation is performed with the same laser system parameters and a sample configuration that was published in previous studies [1, 2]. Specifically, $P = 400 \text{ mW}$, $r_0 = 100 \mu\text{m}$, the laser scan rate is 30 mm/s , and the film melting point is 80°C . For each run, the goal is to quantify how far away in height (z) and in horizontal distance (y) the film has melted away from the edge of the stained cancer cells. Figure 3 shows the simulations for different cases.

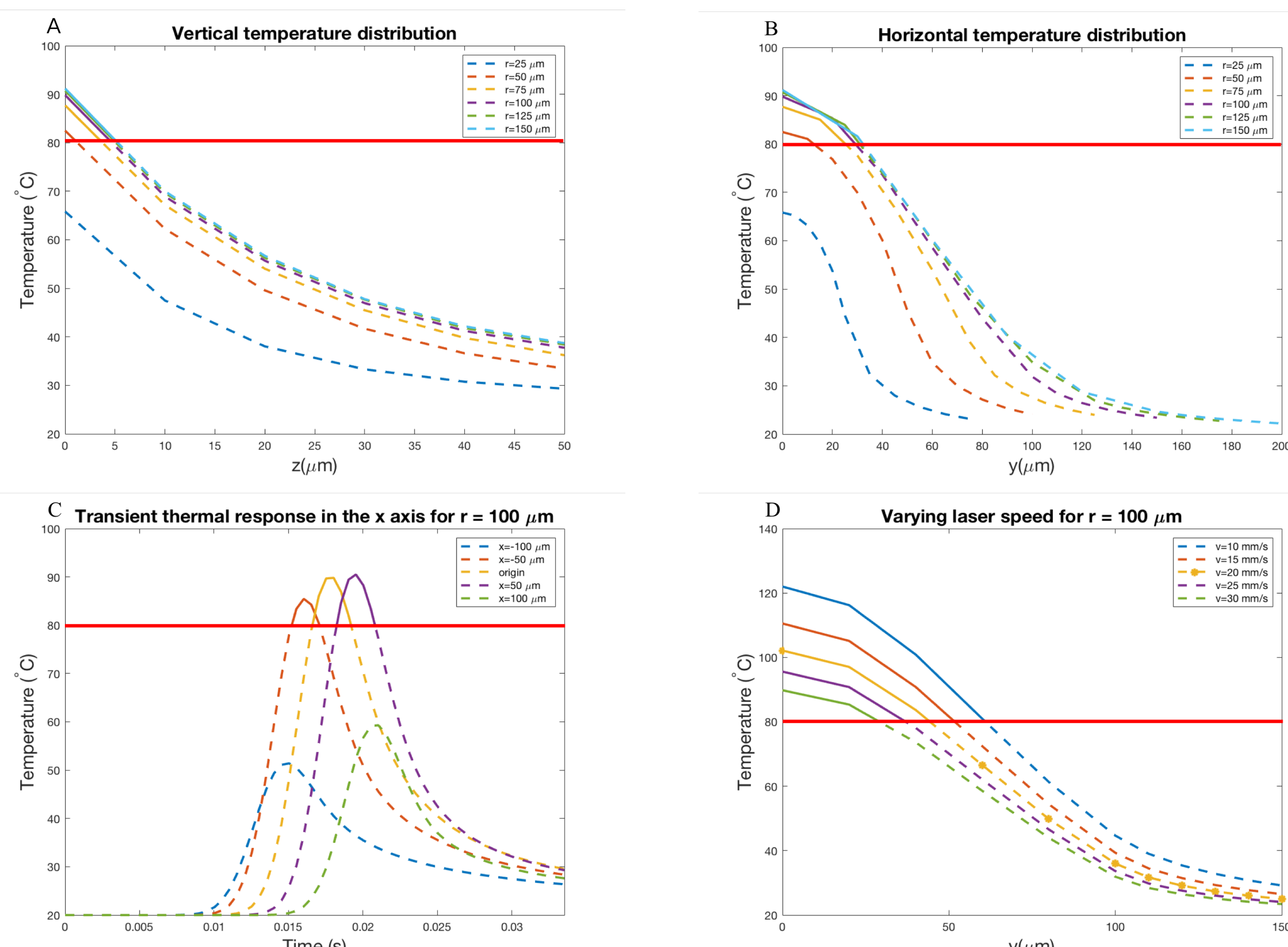


Figure 3 Temperature distribution in the A) z axis and B) y axis. For $r = 100 \mu\text{m}$, C) transient thermal response along the laser traveling path (x axis) and D) temperature distribution at different laser speed.

Conclusions

According to the simulations,

1. at the previously published laser rastering speed of $v = 30 \text{ mm/s}$ the results indicated that the region of the film melted did not adequately cover the cancer cells for all cancer region sizes examined and small cancer cells cannot be procured.
2. the simulations of varying laser speed indicated that a speed of 20 mm/s is a good balance at efficiency of cell retrieval without damaging the cells.
3. the results suggested that a flat-top laser profile is a better choice for optimizing the region of the film melted and avoiding the cells from being burned.

Hence the simulations can be used to understand how to select laser rastering speeds to balance high efficiency (get all the cancer cells) without causing any damage to the cells near center.

Reference

- [1] Michael A Tangrea, Rodrigo F Chuaqui, John W Gillespie, Mamoun Ahram, Gallya Gannot, Benjamin S Wallis, JM Carolyn, W Marston Linehan, Lance A Liotta, Thomas J Pohida, et al. Expression microdissection: operator-independent retrieval of cells for molecular profiling. *Diagnostic molecular pathology*, 13(4):207–212, 2004.
- [2] Jeffrey C Hanson, Michael A Tangrea, Skye Kim, Michael D Armani, Thomas J Pohida, Robert F Bonner, Jaime Rodriguez-Canales, and Michael R Emmert-Buck. Expression microdissection adapted to commercial laser dissection instruments. *Nature protocols*, 6(4):457, 2011.
- [3] Robert F Bonner, Thomas J Pohida, Michael R Emmert-Buck, Michael Anthony Tangrea, and Rodrigo F Chuaqui. Target activated microtransfer, June 11 2013. US Patent 8,460,744.
- [4] Surya C Gnyawali, Yicho Chen, Feng Wu, Kenneth E Bartels, James P Wicksted, Hong Liu, Chandan K Sen, and Wei R Chen. Temperature measurement on tissue surface during laser irradiation. *Medical & biological engineering & computing*, 46(2):159–168, 2008.
- [5] Seth R Goldstein, Philip G McQueen, and Robert F Bonner. Thermal modeling of laser capture microdissection. *Applied optics*, 37(31):7378–7391, 1998.
- [6] K Giering, I Lamprecht, O Minet, and A Handke. Determination of the specific heat capacity of healthy and tumorous human tissue. *Thermochimica acta*, 251:199–205, 1995.
- [7] Goran Torlakovic, Vaneeta K Grover, and Emina Torlakovic. Easy method of assessing volume of prostate adenocarcinoma from estimated tumor area: using prostate tissue density to bridge gap between percentage involvement and tumor volume. *Croatian medical journal*, 46(3), 2005.
- [8] ML Pantelides, Colin Whitehurst, James V Moore, TA King, and NJ Blacklock. Photodynamic therapy for localised prostatic cancer: light penetration in the human prostate gland. *The Journal of urology*, 143(2):398–401, 1990.